

## MIT Open Access Articles

*Extraction of Uranium from Seawater:  
Design and Testing of a Symbiotic System*

The MIT Faculty has made this article openly available. **Please share** how this access benefits you. Your story matters.

**Citation:** Picard, Mathieu, Camille Baelden, You Wu, Le Chang, Alexander H. Slocum. "Extraction of Uranium from Seawater: Design and Testing of a Symbiotic System." *Nuclear Technology* (November 1, 2014): 200-217.

**As Published:** <http://dx.doi.org/10.13182/NT13-144>

**Publisher:** American Nuclear Society

**Persistent URL:** <http://hdl.handle.net/1721.1/93097>

**Version:** Author's final manuscript: final author's manuscript post peer review, without publisher's formatting or copy editing

**Terms of use:** Creative Commons Attribution-Noncommercial-Share Alike



# EXTRACTION OF URANIUM FROM SEAWATER: DESIGN AND TESTING OF A SYMBIOTIC SYSTEM\*

**Mathieu Picard, Camille Baelden, You Wu, Le Chang, Alexander H. Slocum**  
Massachusetts Institute of Technology  
77 Massachusetts Ave, Cambridge, MA, USA

## ABSTRACT

Uranium present in low concentration in ocean water has the potential to greatly augment current fuel reserve for nuclear power generation, but the challenge of extracting it economically remains. Two new designs of seawater uranium extraction systems are proposed in this paper, a stationary system and a continuous system both of which utilize a braided polymer adsorbent. The stationary system simplifies the recovery procedure and it is predicted to produce uranium at \$326/kg. The continuous system is attached to an offshore wind turbine system to eliminate the need for additional mooring and increase the overall energy gathering ability of the wind farm system. This system could maximize the adsorbent yield and achieve a production cost of \$403/kg of uranium.

## KEYWORDS

Uranium, Seawater, Extraction

---

\* Published citation: Picard, M., C. Baelden, Y. Wu, L. Chang, and A.H.Slocum, "Extraction of Uranium from Seawater: Design and Testing of a Symbiotic System," Nuclear Technology, 188 (2), 2014, pp 200-217.

## I. INTRODUCTION

Nuclear fission, along with renewable energies, has the potential to greatly reduce carbon dioxide emissions from power generation. However, a 2011 study by the Organization for Economic Cooperation and Development estimated that at the current consumption rate the global conventional reserves of uranium (7.1 million tonnes) could be depleted in roughly a century.<sup>1</sup> Moreover, as reserves decrease, uranium mining shifts to lower quality sites leading to a higher extraction cost. Recent research efforts and innovations technology improving safety and efficiency of reactors could lead to a renewed demand in nuclear power.<sup>2</sup> A growing nuclear power sector will need access to significant uranium reserves at a reasonable cost of extraction. Conventional uranium reserves can be greatly increased by extracting uranium from seawater. Uranium is present in ocean water in the form of uranyl ions at a low concentration of 3-3.3 $\mu\text{g/L}$ .<sup>3</sup> The amount of uranium in the ocean is estimated at 4.5 billion tonnes, nearly a thousand times the conventional reserves.<sup>4</sup>

Uranium extraction from seawater received significant interest historically. One of the first studies was conducted by Davies et al. in an effort to secure uranium supply for Britain at a time when the production of uranium was uncertain.<sup>5</sup> A recent review from Kim et al. details the state of the art in uranium recovery from seawater as well as the improvement that are needed to make it economically viable.<sup>6</sup> Out of the various separation technologies investigated, uranium adsorption by chelating polymers was found to be the most promising in terms of cost, adsorption capacity and environmental footprint.<sup>7-9</sup> High operating cost, durability or toxicity issues made other techniques such as membrane filtration, coagulation or precipitation not as suitable<sup>10-12</sup>.

The process of passively extracting uranium from seawater using adsorbent polymer starts with deploying the adsorbent in seawater. It remains submerged until the amount of uranium captured approaches the adsorbent capacity. The adsorbent is then eluted in acid solutions of increasing concentration to recover uranium and remove other elements that bonded to the polymer. After regeneration the adsorbent can be reused as its

functional groups have been freed. The output from the elution process then undergoes the same purification and precipitation that is typical for mined uranium to produce yellow cake.

Several marine test of polymer adsorbent have been conducted to evaluate performance, feasibility and cost effectiveness of concepts. The Japanese Atomic Energy Agency (JAEA) first developed a system of buoy floated stacks of adsorbent fabric. Due to the large weight of the mooring equipment, mooring operations were found to account for more than 70% of the cost of this concept.<sup>13</sup> To address this problem a buoyant braid adsorbent made of 10cm polyethylene fibers braided to a polypropylene trunk was proposed. Tamada et al. found that it achieved a reduction of 40% of the cost of uranium recovery compared to the adsorbent stack system.<sup>14</sup> They estimated the uranium production cost of the braid adsorbent system at \$1000/kg of uranium. Sachde and Schneider conducted a thorough cost analysis of this latest JAEA concept and calculated the uranium cost to be \$1230/kg-U.<sup>15</sup> They attributed the difference in cost mostly to their consideration of a 5% degradation of adsorbent capacity per use cycle. In comparison the market price of uranium ranged from a currently low \$91/kg-U to a peak of \$300/kg-U when demand for nuclear power was higher. There is space for improvement in the seawater uranium recovery technology to bring down the cost of production.

The work presented in this article is focused on developing efficient deployment and recovery systems that could utilize the braided adsorbent from JAEA. Its aim is to use the latest development in adsorbent technology and to help close the gap between the current price of uranium recovery from seawater and the price of mining uranium.

Having studied the uranium recovery process and the adsorbent characteristics, the authors propose two concepts. A review of the braid adsorbent-chain concept from JAEA shows that a significant fraction of the cost is spent on deployment and recovery of the adsorbent from the ocean. Indeed a high chain to adsorbent ratio as well as the large number of ships required to operate the system limited the cost effectiveness of the system. To overcome these limitations an alternative stationary system is proposed. A 3D net of braid adsorbent is used to

maximize the adsorbent to anchoring weight ratio. It is recovered by a single ship on which the elution process occurs and then redeployed without the need for a round trip to shore. Though improving the performance of the adsorbent is beyond the scope of this study, adsorbent cost can be reduced by shortening recovery intervals. The kinetics of chelating polymers is such that the rate of uranium collection is highest when the adsorbent load is small. To take advantage of this property, a second concept was created which continuously takes the braided adsorbent line from the ocean through an elution process and then returns it to the ocean allowing control over the harvest period. It is designed to function attached to the base structure of an offshore wind farm. This way offshore mooring costs and the need to find an eligible site are avoided. In addition by collecting uranium it increases the energy output of the wind farm operation making ocean surface utilization more effective.

A first order technical and cost analysis of both continuous and stationary system suggests that they can significantly reduce the cost of recovering uranium from seawater. The stationary system shows promise in minimizing capital and operation cost by providing an efficient adsorbent deployment and recovery system. It achieves a production cost estimated at \$282/kg-U. By reducing the harvest period to maximize adsorbent yield and using an efficient architecture the continuous system is estimated to achieve a production cost of \$446/kg-U. Though the cost analysis resulted in a higher cost for the continuous system, this concept was pursued because it presented several other advantages: potential to optimize the use of future adsorbent with faster kinetics and better durability, symbiotic operation with wind farm removing the need for finding additional offshore sites, scalability from a wind turbine to an entire wind farm. Accordingly, a 1:50 scale prototype of the continuous system was built and tested in a pool to investigate the kinematics of the mechanical system in a fluid environment, and is presented in appendix A. Testing showed that the system could be run continuously in an aquatic environment while remaining stable and was able to sustain currents of medium strengths.

## **II. FUNCTIONAL REQUIREMENTS**

The functional requirements of our collection system of Uranium from ocean water are the following:

- Using amidoxime polyethylene braid adsorbent developed by the Japan Atomic Energy Agency<sup>14</sup>
- System should scale to recover 1200 tonnes of Uranium from seawater per year, enough to supply a 5GW nuclear power plant
- Bring the cost of uranium extraction from seawater as close as possible to uranium mining

### III. ADSORBENT BEHAVIOR

Since a good understanding of the adsorbent behavior is required to design a suitable uranium extraction system, key characteristics of the adsorbent are presented in this first section, namely the recovery rate of uranium and the adsorbent degradation from exposure to acid during the elution process

#### III.A. Recovery Rate

The rate at which uranium can be collected by the adsorbent will depend on its capacity and adsorption kinetics. The capacity of the adsorbent chosen for this system was reported to be 2.85 mg-U/g-ads when tested in a lab environment.<sup>16</sup> Marine test conducted off the coast of Japan showed that a first order kinetic model is able to provide a good match with the uranium adsorption data.<sup>4</sup> This confirms earlier findings from a study by Rudzinski and Plazinski<sup>17</sup> on the uranium adsorption kinetics.

Therefore the concentration of Uranium in the adsorbent ( $C$ ) can be expressed as:

$$C = C_0 \left(1 - e^{-\frac{t}{\tau}}\right) \quad (1)$$

Here  $C_0$  is the capacity of the adsorbent, which was reported to be 2 mg-U/g-ads in seawater,  $t$  is the time of exposure of the adsorbent to seawater and  $\tau$  is the time constant of adsorption. Fitting the marine test data from the Japan Atomic Research Institute<sup>4</sup>, the time constant of adsorption is found to be 15 days.

Because of the nature of the adsorbent kinetics it is possible to increase the recovery rate of uranium by shortening the harvest period. Let's for instance compare the amount of uranium collected over 120 days when the period of uranium recovery from the adsorbent is reduced from 60 days to 30 days. This is illustrated in Fig. 1.

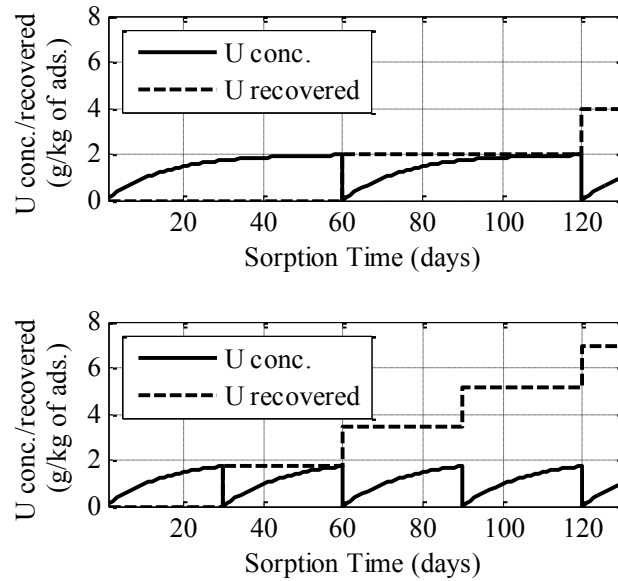


**Fig. 1 Adsorption kinetics, Recovery Period - (top) T=60days; (bottom) T=30 days**

The solid lines represent the concentration of uranium in the adsorbent. It increases following a first order kinetics behavior and then returns to zero after each harvest. The broken lines represent the amount of uranium recovered and each step matches the amount that was extracted from the adsorbent during harvest. For a recovery period of 60 days the adsorbent reached a concentration of 2 gU/kg-ads and a total mass of uranium of 4 g was collected over 120 days (2 harvests). When the recovery period is reduced to 30 days the maximum concentration becomes 1.7 gU/kg-ads leading to a total of about 7 g of uranium collected over 120 days (4 harvests). The difference in adsorbent yield comes from the fact that due to its kinetics most of the uranium is captured in the first 30 days. It is therefore more efficient to have shorter adsorption cycles and to operate the adsorbent at a faster recovery rate of uranium.

Let  $T_h$  be the harvest period, the rate of uranium recovery,  $R$ , is as follows:

$$R = \frac{C(T_h)}{T_h} = \frac{C_0 \left(1 - e^{-\frac{T_h}{\tau}}\right)}{T_h} \quad (2)$$

The recovery rate reaches a maximum as the harvest period approaches zero:

$$\lim_{T_h \rightarrow 0} R = \frac{C_0 \left(1 - e^{-\frac{T_h}{\tau}}\right)}{T_h} = \frac{C_0}{\tau} \quad (3)$$

Figure 2 shows the variation of uranium recovery rate with the harvest period. The final choice of harvest period is a compromise between obtaining the highest recovery rate and minimizing damage to the adsorbent from more frequent elution.

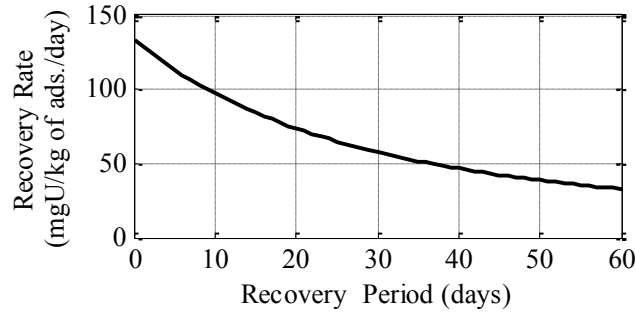


**Fig. 2 Recovery rate of uranium**

### III.B. Degradation

Experimental observation showed that adsorbents can lose as much as 20% of their initial capacity over 5 adsorption/ elution cycles.<sup>18</sup> It is therefore important to account for this degradation of the adsorbent in our analysis.

Exposure to highly concentrated acid is believed to cause damage to the functional groups of chelating polymer adsorbent thus reducing their capacity. To model degradation during elution it can be assumed that the

time the adsorbent is exposed to the acid solution and the solution pH remain constant regardless of the recovery period. This is indeed necessary to make sure that all of the uranium is extracted from the adsorbent. Consequently, the relative loss of adsorbent capacity is assumed to be constant at each elution cycle since the damage to the adsorbent is expected to be the same.

If  $d$  is the relative loss of adsorbent capacity from an elution cycle,  $C_0$  the initial capacity of the adsorbent then the capacity of the adsorbent after one elution cycle  $C_1$  can be expressed as:

$$C_1 = C_0(1 - d) \quad (4)$$

Extending this definition, the capacity of the adsorbent after  $n$  elution cycles can be written as:

$$C_n = C_0(1 - d)^n \quad (5)$$

Using a geometric progression the average capacity of the adsorbent over  $n$  adsorption/elution cycles can be calculated:

$$\bar{C} = \frac{1}{n} \sum_{k=0}^{n-1} C_0 (1 - d_e)^k = \frac{C_0}{n} \left[ \frac{1 - (1 - d_e)^n}{d_e} \right] \quad (6)$$

Figure 3 shows the evolution of adsorbent capacity and average adsorbent capacity with the number of adsorption/elution cycles. The adsorbent was chosen to have an initial capacity of 2 gU/kg-ads and the degradation per cycle was set to 4.4% to match the observation by Seko et al.<sup>18</sup>

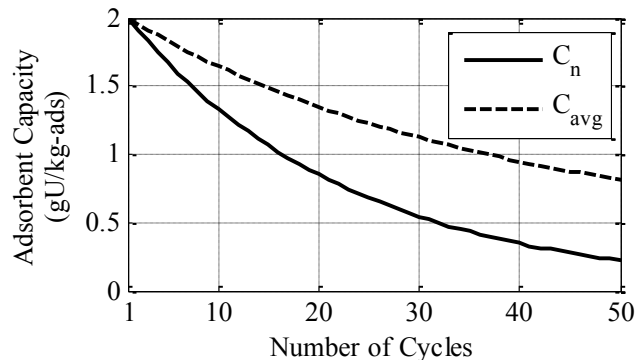


**Fig. 3 Adsorbent degradation**

The solid line shows the evolution of adsorbent capacity whereas the broken line is a plot of the adsorbent average capacity over  $n$  cycles. After 15 adsorption/elution cycles the capacity of the adsorbent dropped to roughly 1gU/kg-ads, half of its original value. The average capacity of the adsorbent over the same 15 cycles is about 1.4gU/kg-ads.

It is evident that degradation from the elution process significantly affects the performance of the adsorbent. Suzuki et al.<sup>19</sup> demonstrated that significant amount of Vanadium was adsorbed alongside the uranium by amidoxime polymers. To extract Vanadium and free the adsorbent functional groups, the concentration of the hydrochloric acid elution solution has to be increased by almost two orders of magnitude compared to what is necessary for uranium extraction<sup>19</sup>. It is therefore likely that most of the elution damage comes from the removal of Vanadium. If a reduction of the adsorbent selectivity to Vanadium could be achieved, the damage to the adsorbent in the elution process could be significantly lowered. This would favor continuous systems since it would reduce the penalty from frequent elution.

#### **IV. ELUTION**

Both systems presented in the present paper for recovering the adsorbent are running an on-site continuous elution process. As the flow rate of adsorbent through the elution system can greatly differ from previously suggested systems, it is important to understand how this system scales.

The elution is a chemical process in which the adsorbent reacts with hydrochloric acid and nitric acid in two separate stages.<sup>14</sup> The two outcomes of the elution are a solution of acid and earth metal ions including uranium and fresh adsorbent for reuse. This solution is further purified to separate uranium out. In the JAEA system, the braided adsorbents are shipped from the deployment site to a land facility where elution and purification is performed. This reduces the recovery system uptime which can be remedied by performing elution at the deployment site and shipping the produced uranium solution to a land facility for purification.

#### **V. MOORING AND RECOVERY**

Two designs are presented for the mooring and recovery of the adsorbent. The first system is a platform attached to an off-shore wind turbine with the adsorbent cycling around it. This concept allows the adsorbent to be cycled at the optimum speed without increasing significantly the capital and operational costs, but incurs higher capital expenses. The second concept is a three-dimensional net that would be recovered by a single ship transporting the elution plant. This concept reduces the capital expenses to a minimum, but a faster cycle time of the adsorbent results in a larger system.

In this section, engineering first order calculations are presented for both concepts to show the technical feasibility. While some representative numbers are given, the calculations are parametric in order to allow for optimization of the total cost of the system. Trade-offs for both systems are described in the economic section.

## V.A. Strategy 1: Stationary 3D Net

The goal of the three-dimensional net is to reduce to a minimum the size of the recovery system for the amount of adsorbent collected. The system is inspired from the concept proposed by the Japan Atomic Energy Agency<sup>14</sup>, but greatly reduces the amount of chains and ships needed. The concept, shown in Fig. 4, is a net of adsorbent attached to two chains and masses lying at the bottom of the ocean. A single ship continuously recovers the net, runs it through the elution process and replaces it at the bottom. The number of braids in parallel in the net is chosen so that the ship can harvest all the net during the selected harvest period at the recovery velocity ( $v_a$ ) taken 4 m/min, and produce 1200 tonnes of uranium per year.

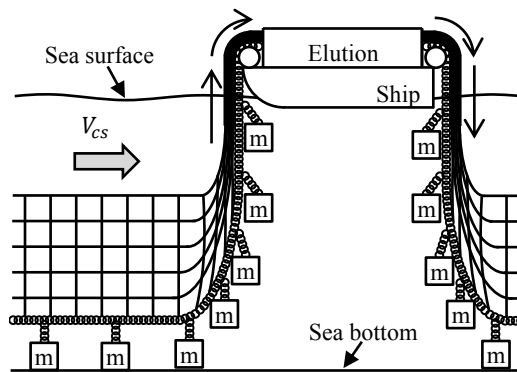


**Fig. 4 Side view of the 3D net mooring and recovery system**

The 3D net is composed of a series of braided lines in parallel ( $N_p$ ), 165 in the baseline design, with some interconnecting braided lines, as shown in Fig. 5. The height of the net ( $H_n$ ) is 60 m to leave sufficient room above, assuming a depth ( $H$ ) of 100 m, as shown in Fig. 6.

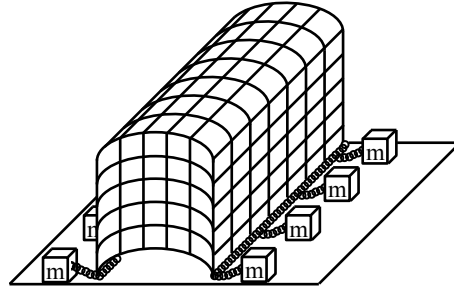


**Fig. 5 Section of the 3D net (number of braided lines is reduced and braided lines inside the net are not shown for clarity)**

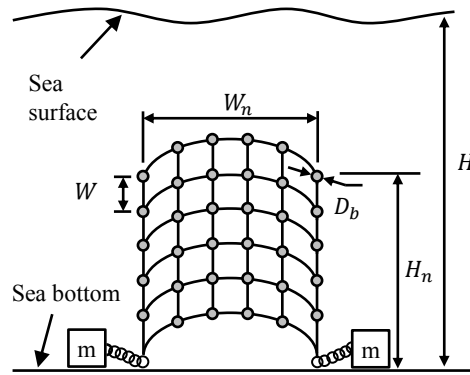


**Fig. 6 Cross-section of the 3D net without current (number of braided lines is reduced for clarity)**

The spacing between the braids ( $W$ ) is 3 m to leave sufficient room for marine life to move freely and to avoid reducing the local concentration of uranium. The width of the net ( $W_n$ ) is calculated based on the spacing and the total number of braids, which result in a baseline value of 21 m. In the shown construction, for every parallel section of braid there is two braids perpendicular to it at the knot, one upward and on towards the other side of the net, so the total number of braids per number of parallel braids is 3, defined here as the net construction factor ( $N_b$ ).

The net is attached to one chain on each side used to recover the net and to provide part of the weight needed to keep the net at the bottom. The remaining weight needed is provided by concrete blocks attached to

the chain. During the harvest, the complete assembly is brought aboard the ship, the adsorbent passes in a continuous elution process, and the net is replaced behind the ship.

An important concern is that the concentration of uranium in the water remains sufficiently high throughout the net and from one net to another. The minimum velocity needed so that the mass fraction of uranium leaving the net is minimally affected by the uranium adsorbed is estimated by a simple control volume analysis of one row of adsorbent (Fig. 7). The minimum velocity can be calculated from a mass balance of uranium:

$$\rho_w W V_w (w_{U,in} - w_{U,out}) = m'_b N_W N_b R \quad (7)$$

in which  $\rho_w$  is the density of water,  $V_w$  is the velocity through the net,  $w_{U,in}$  and  $w_{U,out}$  are the mass fraction of uranium in sea water entering and leaving the net,  $m'_b$  is the mass of adsorbent per meter of braid,  $N_W$  is the number of braids along the width of the net, and  $R$  is the recovery rate as defined in the adsorbent behavior section. The minimum velocity through the net is 6 mm/s, for the concentration of uranium leaving the net to be 90%. It is reasonable to assume that a location can be found with a velocity higher than this minimum value.

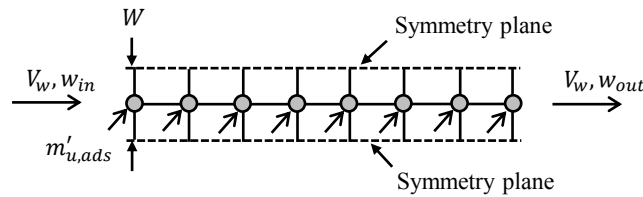


**Fig. 7 Control volume on one row of adsorbent in the net**

The spacing between the nets ( $W_g$ ) is estimated based on the assumption that the volume of water for one net should be enough to supply the amount of adsorbed uranium in a year. The spacing between two nets should be 3 km, based on a depth of a 100 m. In the baseline design the total length of 3D net needed is 300 km, which leads to a total area of 900 km<sup>2</sup>, which is on the same order as the 1000 km<sup>2</sup> needed for the JAEA concept.<sup>14</sup>

The design variables in sizing the system around the 3D net is the diameter of the chain link ( $d_c$ ) and the mass of concrete needed on both side of the net per unit length of chain ( $m'_M$ ). The design criteria are: (1) the chain must be able to sustain the tension to recover the net, and (2) the net must remain in place at the bottom when a cross-flow is applied, deforming the net from its buoyant position to a position aligned with the flow.

The tension in the chain ( $T$ ) when recovering the net is given by

$$T = H \left( \frac{F'_T}{4} + F'_M + F'_C - \frac{F'_B}{2} \right) \quad (8)$$

$$F'_T = \frac{1}{2} \rho_w V_{cs}^2 W_n C_D$$

in which,  $H$  is the depth of the net,  $F'_T$  is the transversal drag force on the net per unit length of net due to cross flow,  $F'_M$  is the effective weight of the masses per unit length,  $F'_C$  is the effective weight of the chain,  $F'_B$  is the buoyancy of the net per unit length,  $V_{cs}$  is the current at the surface,  $W_n$  is the width of the net, and,  $C_D$  is the drag coefficient, taken as unity in this first order calculation.

For the drag, as the net describes a curve when subjected to a cross-flow, the end of the chains becomes almost parallel to the surface. Therefore, the transversal drag force is compensated by the tension in the two chains at the top and the two chains at the bottom. The drag force is calculated with the width of the net as this is the maximum width of net that can be exposed to the cross-flow when the net is replaced in the water.

Assuming the maximum allowable tension is half the proof load, the tension ( $T$ ) in Newtons of a R3 grade can be related to its nominal diameter of the chain by<sup>20</sup>

$$T = 7.8 \times 10^6 d_c^2 (44 - 80d) \sim 3 \times 10^8 d_c^2 \quad (9)$$

in which the nominal diameter of the chain is taken in meters. The expression is simplified by using the baseline diameter to evaluate the second part of the equation.

The second design criterion concerning the resistance to a cross-flow at the bottom of the sea is met when the friction force balance the drag force of the collapsed net (Fig. 8):

$$\frac{1}{2} \rho_w V_{cb}^2 H_D C_D = 2 \mu \left( F'_C + F'_M - \frac{F'_B}{2} \right) \quad (10)$$

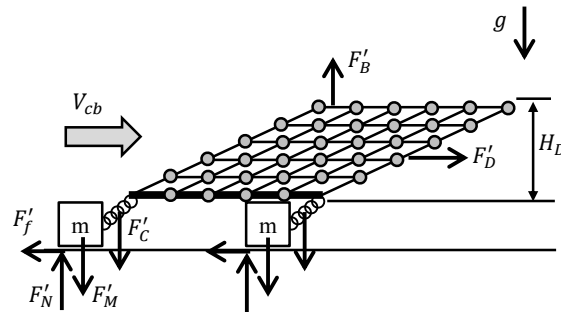


**Fig. 8 Cross-section of the 3D net submitted to a cross-flow**

The left hand side of equation 10 represents the drag force, whereas the right hand side is the resisting friction force. Here  $\mu$  is the friction coefficient between the chain and the masses with the ocean floor taken to be 0.5 in this analysis, and  $H_D$  is the height of the collapsed net.

As the net aligns itself with the cross-flow similarly as a cross-flow at the bottom (Fig. 8), the frontal area is given by approximately two times the height of the braided lines stacked on each other:

$$H_D \approx 2 D_b N_h \quad (11)$$

in which  $D_b$  is the diameter of one braided line, and  $N_h$  is the number of braided lines along the height of the net. Solving simultaneously eq. (8) and (10) results on a chain diameter of

$$d_c = \left( \frac{H\rho_w C_D}{1.2 \times 10^9} \left[ \frac{V_{cs}^2 W_n}{2} + \frac{V_{cb}^2 H_D}{\mu} \right] \right)^{1/2} \quad (12)$$

From eq. (12) one can see that the diameter of the chain depends on the velocity of the cross-flow current both at the surface and at the bottom of the sea, chosen conservatively here to be respectively 2 and 1 m/s. It is also clear that operating the system in a location with small current reduces directly the size of the chain necessary. The presented baseline design results in a chain diameter of 7.1 cm. The mass of the chain can be calculated by<sup>20</sup>

$$m'_c = 2.19 \times 10^4 d_c^2 \quad (13)$$

The mass of chain in the baseline design is 110 kg/m. The mass needed to maintain the net at the bottom is given by

$$m'_M = \frac{\rho_M}{g(\rho_M - \rho_w)} \left( \frac{F'_D}{\mu} + \frac{F'_B}{2} - F'_C \right) \quad (14)$$

The mass of concrete in the baseline design is 378 kg/m, which is reasonable as it is on the same order as the mass of the chain. The concrete mass is distributed along the net by attaching concrete blocks to the chains.

At the bottom of the net, a cable is used to make a connection between the two chains, as identified by a larger line in Fig. 8. This cable is made stronger to support the tension in all the vertical braided lines created by a cross-flow at the bottom of the sea. The lowest cable should be able to sustain a tension ( $T_L$ ) of

$$T_L = \frac{1}{2} \rho_w V_{cb}^2 C_D H_D W \quad (15)$$

and its diameter ( $d_L$ ) is given by

$$d_L = \left( \frac{4 FS_L T_L}{\pi \sigma_{yL}} \right)^{1/2} \quad (16)$$

in which  $FS_L$  is the safety factor of the cable, taken to be 3 for this analysis, and  $\sigma_{yL}$  is the tensile strength of the cable. Resulting wire rope cable diameter is 1.0 cm for the baseline design. The total tension in the lowest support is divided into all the vertical supports. Thus the polypropylene core of the adsorbent should be a minimum of 1.0 cm to support the tension.

The size of the elution plant is scaled from the calculation made by Sachde<sup>15</sup>. The elution tank volume is scaled based on the mass flow rate of adsorbent. The chemical tanks are scaled based on the mass flow rate of uranium eluted. Two tanks with the same size as the chemical tanks are added to collect the elution solution that is brought back to the shore to the purification and precipitation plant.

## **V.B. Strategy 2: Symbiotic Offshore Structure**

The second strategy is a continuous system designed to operate in symbiosis with existing offshore structures thus eliminating the need for additional site and mooring. By adding uranium extraction it increases the energy harvesting output of the existing offshore operation. As shown in Fig. 9, the system consists of an on-site elution plant and a series of automatic conveying belts, which transfer adsorbent between seawater and the elution plant.

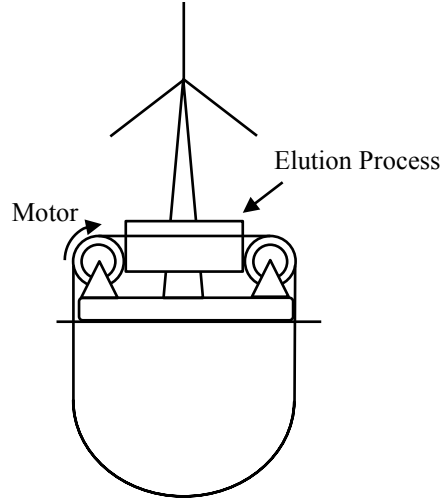


**Fig. 9 Continuous system concept**

The variable cost of extraction of uranium from seawater can be reduced through optimizing the cycling period of the adsorbent to obtain a larger yield. The system is designed to maximize the amount of adsorbent per offshore structure and limit the capital cost. Each system is sized to extract uranium at 1.2 tonnes per year, a rate sufficient to fuel the production of 5 MW of electricity in an onshore nuclear plant which would be fed by many such systems. Therefore it matches the capacity of a typically envisioned offshore wind turbine.

Two designs are proposed to maximize the volume of adsorbent circulating in the continuous system. The first one as shown in Fig. 10 (a) consists of a grid of braided adsorbent lines attached to two vertical cables. The alternative design shown in Fig. 10(b) replaces the belt by multiple cables surrounded by braided adsorbents. The adsorbent density for both designs can be compared. The belt design carries 41 m of adsorbent per meter of belt if a grid spacing of 1 m (necessary to ensure good contact between the adsorbent and sea water) and a belt width of 20 m. Five separate cables can carry 41 m of adsorbent per meter of assembly if 6 braided lines are attached per node. The braided lines would be 5 m long for spacing of 3 m between the cables. The grid concept is selected as it can be more easily run over the pulleys of the continuous system described here

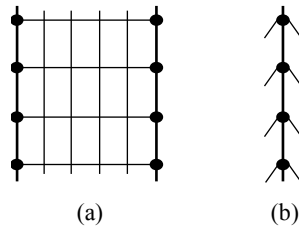


**Fig. 10 Two designs of the belt. Thick lines represent high strength cable and thin lines represent adsorbent braided lines. The cables can be replaced with bead belt or chains.**

The adsorbent assembly (belt or cables) can either be run around a single turbine supporting structure (Fig. 9) or in between two turbines (Fig. 11). While connecting multiple turbines would make better use of the space between turbines of an onshore wind farm there is also a concern that drag on the adsorbent belt could pull turbines together and damage their structures. Moreover the single turbine layout allows scaling from one turbine to an entire wind farm and provides better access to the turbines, and is thus chosen as the most suitable layout.

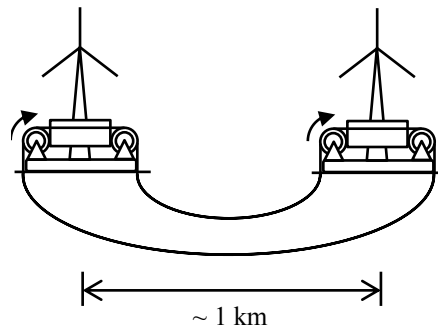


**Fig. 11 Layout (a) of the belt**

Figure 12 shows a solid model of the selected concept which was used to build the scale model for pool testing. A circular platform is attached to the mast of the turbine. The adsorbent belt forms multiple loops that come up on the platform and are run under seawater. This increases the density of adsorbent around the turbine. The outer cables of the belt are driven by a system of shafts and pulleys rotating at the same speed. The lower platform has rollers which guide the adsorbent belt, prevent entanglement and make sure the loops maintain the

same length. Every full revolution the belt of adsorbent goes through an elution cycle which is located on the top platform.

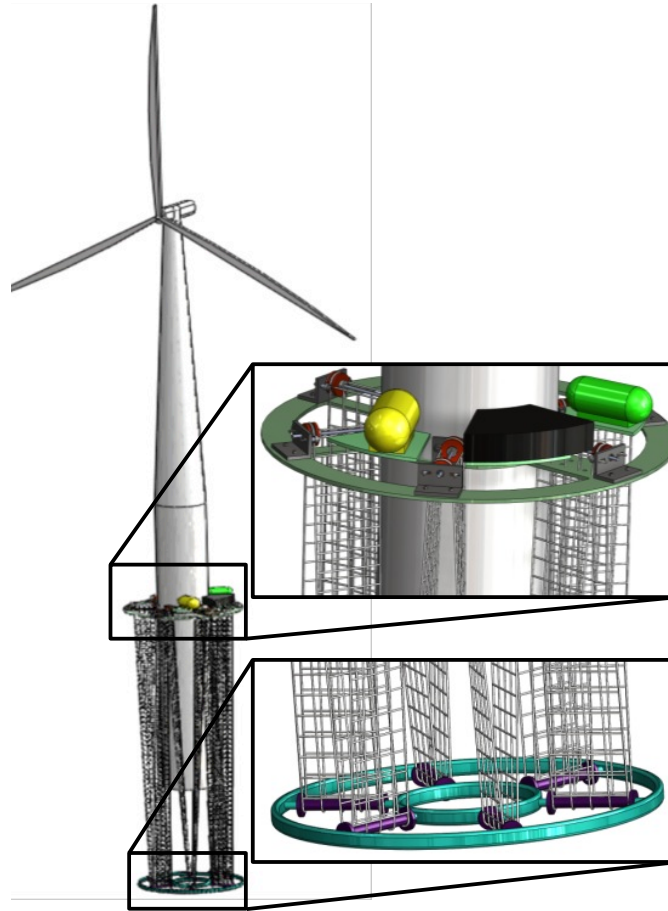


**Fig. 12 Layout (b) of the belt. For easiness to see, only 6 loops of belt instead of 20 are drawn in the figure.**

To satisfy the 5 MW per system power output requirement, a system of 20 loops of 100 m deep each need to be running at 38 days per cycle. The total belt length is 4000 meters. The length of each loop can be longer as long as the depth of water at the location allows. The central reservoir on Fig. 12 represents the space required for the elution process. Two storage tanks store enough chemicals to feed the elution process for up to a month before a crew comes to collect the harvested uranium and refill the tanks. Sizing of the elution process was estimated by scaling down the mass flow rate of adsorbent from reference elution plants.<sup>15</sup>

Sea currents impose drag force on the system, and load carrying components are sized to sustain the maximum possible drag. Starting from the bottom, the bottom platform with 20 rollers prevents the loops from being entangled. It is made out of stainless steel tubes and HDPE rollers slide-fit on to the tubes to minimize friction force against the belts. This bottom platform is attached to the anchor system of the wind turbine which allows it to move up and down to mitigate the drag force from strong currents. This platform weighs around 3 tonnes.

Steel wire rope is chosen to carry the adsorbent belt for its strength and flexibility. Similar to the one in the 3D net system, a cross flow current ( $V_{cs}$ ) of 2 m/s is assumed, which generates a drag force ( $F_D$ ) on each half loop of

$$F_D = \frac{1}{2} \rho_w V_{cs}^2 C_D D_b N_p N_b H_l \quad (17)$$

in which  $H_l$  is the length of the loop, and the other variables are as defined in the 3D net section. For a 2D belt the construction factor ( $N_b$ ) is 2. The bottom platform moves up to allow the belt to form a curve, and it is assumed there is an angular offset ( $\theta_n$ ) from its vertical position at both end of the belt, taken to be  $60^\circ$ , as shown in Fig. 13.

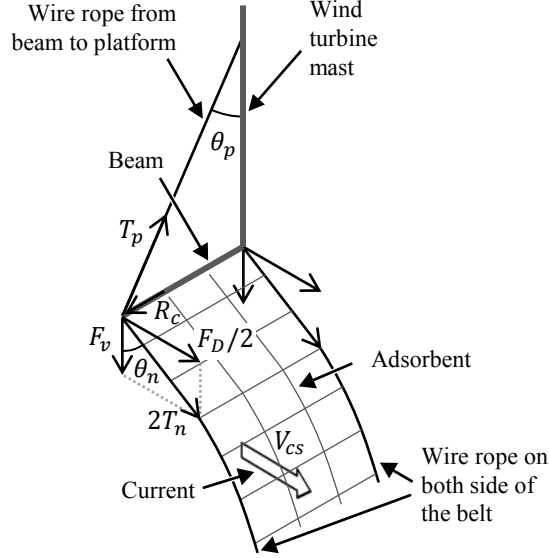


**Fig. 13 Modeling the cantilever beam structure in the top platform**

The diameter of the wire rope ( $d_n$ ) needed on both side of the belt can be calculated from the tension force supported

$$d_n = \left( \frac{F_D \cdot FS_c}{\pi \sigma_{yc} r_\rho \sin(\theta_n)} \right)^{1/2} \quad (18)$$

in which  $FS_c$  is the factor of safety for the wire rope (2 in the presented analysis),  $\sigma_{yc}$  is the tensile strength of the wire rope (1800 MPa), and  $r_\rho$  is the filling ratio of the wire rope as compared to a full steel section ( $\sim 0.63$  from the manufacturer specification). The wire rope diameter needed in the nominal design is 3.3 cm.

Square tubes are used to construct the top platform, one below each pulley shaft assembly. They support all devices on the platform and the belt load. To reinforce the structure, a steel wire rope diagonal is added to the free end of the beam, at an angle  $\theta_p$  from the vertical, chosen to be  $30^\circ$  to provide sufficient support while not interfering with the turbine blades. To avoid buckling, the beam width ( $b$ ) can be calculated by

$$b = \left( \frac{12F_D \tan(\theta_p) L^2}{\tan(\theta_n) \pi^2 E (1 - (1 - 2x))^4} \right)^{1/4} \quad (19)$$

in which  $L$  is the length of the beam,  $E$  the Young's modulus for steel, and  $x$  the thickness-to-width ratio of the beam. A beam of 21 m long, 38 cm wide and 7.6 mm thick satisfies the requirement for the nominal design. Adjusting the design to standard sizing or replacing the beam by a truss would be needed in next design stages, but this estimation allows for an estimation of the cost of the additional structure.

The needed diameter of the wire rope ( $d_p$ ) supporting the end of the beam is calculated to be 3.6 cm using the following equation:

$$d_n = \left( \frac{2 F_D \cdot FS_c}{\pi \sigma_{yc} r_p \cos(\theta_p) \tan(\theta_n)} \right)^{1/2} \quad (20)$$

A single motor is used to drive all 20 pulleys at same time. At the rate of 38 days per cycle, this 4000-meter-long belt is being conveyed at 8 cm/minute. Even if the drag of each perpendicular braided line in the belt is modeled as the flow over a cylinder, the total amount of power required to overcome the drag force at such a low speed would be around 20W. However, if we size the motor such that the belt experiences no tension in the elution plant, the additional power requirement will be the product of tension force and velocity, which is 800W. The total power requirement for the motor is 820W.

## VI. ECONOMICS

In order to evaluate both concepts against each other and the concept proposed by the JAEA, a cost analysis is presented based on the methodology described by Sachde<sup>15</sup>. The total cost of the system is divided in three

sections: (1) the adsorbent, (2) mooring and recovery (M&R) of the adsorbent, and (3) elution, purification and precipitation (EPP). Adsorbent production cost is assumed to be 5.39 \$/kg-ads based on Sachde's analysis.<sup>15</sup> The total amount of replacement adsorbent needed per year is calculated separately for the two concepts based on 1200 tonnes of uranium collected annually, the effective capacity of the adsorbent, the number of cycles per year, and the maximum number of cycles. Capital and operational costs for the other two sections are evaluated separately for the two concepts, as they differ greatly in size.

The general methodology for the capital costs is to cost the principal equipment. A delivery cost of 10% is added to all equipment and a contingency of 10% is also added. An interest rate of 10% is used and the equipment is amortized over 15 years. An interest rate of 6.5% is accounted for in the construction period.

M&R operational costs cover labor, fuel and electricity, and fabrication of the net for the replaced adsorbent. Maintenance and other operational costs are included by adding 4% of the initial capital cost every year.

EPP operational costs include labor, utilities, and chemicals. A disposal fee of 0.36 \$/kg adsorbent is included at the end of the adsorbent life time. A contingency of 10% is added to all operational costs.

The methodology is validated by evaluating the costs of the JAEA concept and compare with the results obtained by Sachde.<sup>15</sup> All costs and cost equation are given in 2013 US\$, unless mentioned otherwise. Costs were converted to 2013 US\$ from their original data using the Consumer Price Index.<sup>21</sup>

## **VI.A. 3D Net Concept Costs**

The main equipment for the mooring and recovery of the 3D net concepts are: (1) a ship, (2) four anchor windlasses, (3) chains, and (4) concrete blocks.

For strategy 1, elution ship costs are estimated from the empirical relation from Culliane and Khanna<sup>22</sup> developed based on ship costs from 2800 to 84,000 DWT:

$$\ln(\text{ship price}) = 4.8097 + 0.759 \ln (\text{DWT}/14) \quad (21)$$

in which the ship price is in thousands of 1996 US\$. The tonnage of the ship is taken to be two times the total weight of the chemicals, the elution tank full of solution, and 3D net assembly on the boat. Baseline ship tonnage is thus 16,000 DWT.

The four anchor windlasses and other equipment on the ship, except for the elution plant, are conservatively estimated to be 1/2 of the ship price.

Chain cost is evaluated based on extrapolated costs by Sachde and can be simply expressed as

$$\text{chain cost} = \text{chain length} \times 40.91 \text{ \$/m} + \text{chain mass} \times 1.37 \text{ \$/kg} \quad (22)$$

Concrete cost is evaluated with a price per weight of 200 \\$/tonne.

Operational costs for M&R include: (1) labor, (2) fuel, and (3) fabrication of the replacement net. Labor costs is evaluated based on Culliane and Khanna<sup>22</sup> empirical data that the crew size for a ship larger than 11,200 DWT is 24. To include the operation of recovering the net, the crew is doubled. Labor costs for M&R is evaluated with 1 captain at a salary 114.6 k\\$/yr and 47 sailors at a salary of 61.2 k\\$/yr, including 54% added for benefits.<sup>23</sup>

Fuel cost is evaluated based on a use of 20% of the ship engine capacity and the power required to drive the four anchor windlasses. Engine capacity in horsepower (BHP) is calculated from a correlation developed by Cullinane and Khanna<sup>22</sup>

$$\ln(\text{BHP}) = 2.6308 + 0.967 \ln (\text{DWT}/14) \quad (23)$$

Power to drive at the engine one anchor windlass ( $P_{aw}$ ) is calculated by

$$P_{aw} = \frac{Tv_a}{\eta_{aw}} \quad (24)$$

in which  $\eta_{aw}$  is the combined efficiency from the engine to the chain, taken 75% in the current analysis. Fuel consumption is based on a specific fuel consumption of 0.219 kg/kWh<sup>24</sup> or 0.084 gal/bhp-hr. Cost of the fuel is taken at \$0.79/L (\$2.99/gal). Net fabrication costs are approximated to be \$10/m net.

Elution/purification/precipitation (EPP) costs level of detail in this analysis is chosen to show the difference between the on-shore and off-shore elution. EPP capital cost includes: (1) tanks for storage and elution, (2) elution equipment, (3) purification and precipitation capital costs. Acid storage tanks of the same size as the on-shore plant are kept on-shore to avoid too frequent refilling. Storage tanks are also added on the boat. Based on a bi-weekly return to the shore, the volume of the tanks on the boat is reduced by a factor of about 9. Cost of the tank is scaled by a two-third power of the volume as cost scales with area. A third set of tanks which has the same size as the total acid storage tanks is added to store the products of the elution until the ship return to the shore. A downtime of 12 h every time the ship goes back to the shore is added to a 15% down time when at sea. Equipment for elution is kept at the same as the previous evaluation. Capital cost of the purification and precipitation section is also kept the same.

EPP operational cost includes: (1) elution labor, (2) purification and precipitation labor, (3) chemicals, (4) utility costs, and (5) disposal. All of them, except disposal, are taken from the previous analysis. Disposal cost is evaluated at 0.38 \$/kg of adsorbent replaced.<sup>15</sup>

## VI.B. Symbiotic Concept Costs

Symbiotic concept costs are similarly evaluated. The main difference consists in the costing of the platform attached to the wind turbine, the number and size of ships, and the elution system.

Capital M&R costs include: (1) ships, (2) cables, (3) platform structures, (4) drive system, and (5) bottom platform. Ship costs are evaluated from the previously presented correlation for a 300 DWT size. The number of boats required is selected to be able to visit each platform once a month to replace the chemicals, collect the elution solution, replace the adsorbent if needed, and do the maintenance. It is estimated that one ship can visit one platform per day. Cable cost is calculated based on and a price from the manufacturer of  $\$3.23/(\text{m}\cdot\text{cm})$  multiplied by the diameter of the cable and the total length needed. Platform structure cost is based on the total weight of beam needed times  $\$2.5/\text{kg}$  for the steel, totaling  $\$110\text{k}/\text{platform}$ . Drive system cost is estimated at  $\$5\text{k}$  per shaft assembly, including the driving pulleys, sprocket and chain. An amount of  $\$10\text{k}/\text{platform}$  is added for the motor and gearbox. Finally, the bottom platform cost is estimated based on the cost of stainless steel needed for the structure as well as HDPE for the roller. Total bottom platform cost is estimated based on 50% material cost, so the 50% manufacturing cost is added, totaling  $\$10\text{k}/\text{bottom platform}$ .

Operational M&R costs include: (1) fuel, (2) labor, (3) net fabrication. A crew of 9 sailors and 1 captain is estimated per ship. Salary and fuel cost is estimated with the same method as the 3D net concept. Fabrication of the net is estimated at  $\$1/\text{m}$ .

EPP capital costs include: (1) storage tanks, (2) elution tank, (3) other elution equipment, and (4) purification and precipitation section. Storage tank and elution tank costs are evaluated from a correlation based on data from Peters<sup>25</sup> for horizontal stainless tanks:

$$\text{cost tank} = 6812 V_{\text{tank}}^{2/3} + 4144 \quad (25)$$

in which the cost is in \$ and  $V_{tank}$  is the volume of the tank in  $m^3$ . A fourth tank is also added to store the products of elution. Other elution equipment is roughly estimated to \$25k/platform. Purification and precipitation capital costs are again kept the same as the JAEA concept. EPP operational costs are kept the same as the 3D concept.

### **VI.C. Cost Results**

For both concepts, the harvest period is optimized, and the minimum cost is found to be at 6 harvests per year for the 3D net concept, and the symbiotic concept optimum is at 10 harvests per year. The maximum number of cycles before adsorbent replacement is limited to 18 to be on the conservative side, although a larger number would reduce the cost. Results of the cost analysis are shown in Table 1. The discounted cash flows are not taken into account in this analysis. To make a fair comparison, the JAEA concept cost breakdown is also shown without the discount rate.

**Table 1 Cost comparison of the two strategies to the JAEA concept for 1200 tonnes of uranium annually (in 2013 US\$)**

	JAEA concept <sup>14</sup> (Sachde cost analysis <sup>15</sup> )		Strategy 1: 3D Net		Strategy 2: Continuous Symbiotic	
	\$	\$/kg-U	\$	\$/kg-U	\$	\$/kg-U
<b>Adsorbent</b>	<b>651.5 M/yr.</b>	<b>542.95</b>	<b>291.3 M/yr.</b>	<b>242.77</b>	<b>330.3 M/yr.</b>	<b>275.28</b>
<b>Mooring and Recovery</b>						
<b>Capital cost</b>						
Ship	616.4 M	67.53	33.9 M	3.71	37.8 M	4.14
Chain/cable	1728.3 M	189.35	107.1 M	0.93	52.5 M	5.75
Recovery equipment	-	-	16.9 M	1.86	147.3 M	16.14
Additional mooring	-	-	34.5 M	3.78	-	-
<b>Total capital M&amp;R (incl. delivery and contingency)</b>	<b>2837.0 M</b>	<b>310.83</b>	<b>222.5 M</b>	<b>25.50</b>	<b>287.5 M</b>	<b>31.50</b>
<b>Operational cost</b>						
Fuel	30.7 M/yr.	25.58	6.5 M/yr.	5.45	2.3 M/yr.	1.89
Labor	146.2 M/yr.	121.86	2.5 M/yr.	2.08	14.0 M/yr.	11.63
Site rental	2.4 M/yr.	2.01	2.4 M/yr.	2.01	-	-
Net material and fab.	-	-	1.1 M/yr.	0.94	1.4 M/yr.	1.14
Maintenance and other	104.1 M/yr.	86.75	8.9 M/yr.	7.42	11.5 M/yr.	9.58
<b>Total oper. M&amp;R (incl. contingency)</b>	<b>311.8 M/yr.</b>	<b>259.83</b>	<b>23.6 M/yr.</b>	<b>19.68</b>	<b>32.0 M/yr.</b>	<b>26.67</b>
<b>Total M&amp;R</b>		<b>570.66</b>		<b>45.57</b>		<b>58.17</b>
<b>Elution/Purification/ Precipitation</b>						
EPP capital cost (incl. delivery and contingency)	36.1 M	3.96	46.2 M	5.06	182.9 M	20.04
EPP operational cost (except disposal)	15.7 M/yr.	13.12	14.0 M/yr.	10.72	21.7 M/yr.	18.07
Disposal cost	43.5 M/yr.	36.26	19.5 M/yr.	16.21	20.7 M/yr.	17.23
<b>Total EPP</b>		<b>53.34</b>		<b>26.94</b>		<b>59.55</b>
Interest during construction	523.2 M	57.32	48.37 M	5.30	91.6 M	10.04
<b>Total</b>		<b>1224.26</b>		<b>325.85</b>		<b>403.03</b>

Both systems presented in this paper offer an important cost reduction compared to the JAEA concept. This is made possible by a significant reduction in M&R costs. In addition to reducing the total cost, a low cost M&R system allows cycling the adsorbent faster without important penalty in M&R cost. In the JAEA concept,

the adsorbent is left in the water 60 days to become saturated in uranium. Reducing the time between harvests would decrease the amount of adsorbent needed by increasing the recovery rate, as shown in Fig. 2. However, it would also rapidly increase the number of ships needed and labor cost and would therefore be less profitable. On the other hand, the optimum cycle time for the two concepts presented in this paper is about two times faster because of the low M&R cost, which leads to a reduction of the amount of adsorbent needed and thus the adsorbent cost. In other words, a more effective use of the same adsorbent in the concepts proposed here leads to about 50% cost reduction.

In particular, the 3D net system the adsorbent cost is reduced by 55% and the M&R system cost is reduced by more than 90% compared to the JAEA concept. EPP cost is similar to the JEAE concept, except for the disposal cost which is reduced proportionally with the adsorbent replacement cost. The overall uranium harvesting cost is reduced of 74%, to a value of \$326/kg-U, which is slightly below the maximum market price that uranium reached in 2007 corrected for inflation.

For the symbiotic concept, the adsorbent cost is reduced by 49%. The difference with the 3D net concept is that the optimum number of harvest per year is higher leading to more degradation and thus replacement costs. Although higher than the 3D net concept, the M&R costs are reduced by 90% compared to the JAEA concept. One important disadvantage of the symbiotic system is its higher elution costs, which is dominated by the cost of the tanks. The cost of the tanks is proportional to the amount of material, and thus their area. Therefore, if a large tank with a given volume is subdivided in  $N$  tanks containing in total the same volume, the cost is multiplied by  $\sim N^{1/3}$ . As one elution plant is subdivided on 615 platforms, this explains most of the difference between the elution systems of the continuous concept and of the fixed 3D net concept. Total price of uranium, evaluated at \$403/kg-U, is close to the maximum market price of 2007.

The effect of the number of harvests per year is shown in Fig. 14 for the 3D net (annual production constant: 1200 t of U). M&R costs reduce rapidly with the number of harvests as the total length of the 3D net decreases.

When the adsorbent costs start raising it quickly dominates the cost and set the optimum harvest number to 6 per year. Again for the 3D net, Fig. 15 shows the specific cost of uranium as a function of the number of cycles before adsorbent replacement. The cost decreases quickly and then is relatively constant, as the decrease in adsorbent cost is balanced by an increased in M&R cost. Operating the adsorbent for 40 cycles before replacing the adsorbent would lower the cost to \$251/kg-U.

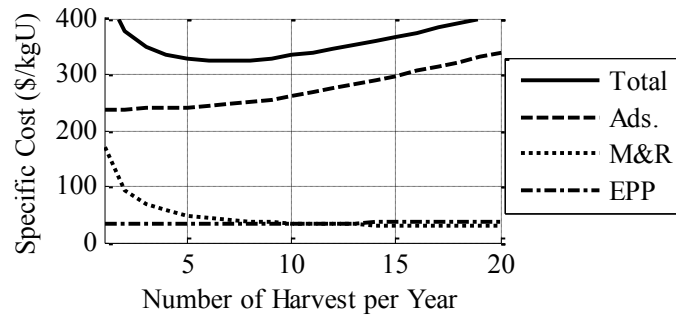


**Fig. 14 Specific Cost for the 3D net concept as a function of the number of harvests per year (18 cycles before replacement of the adsorbent)**

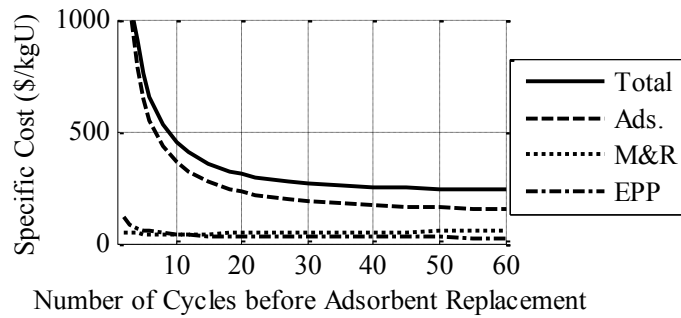


**Fig. 15 Specific Cost for the 3D net concept as a function of the number of cycles before replacement of the adsorbent (6 harvests per year)**

The symbiotic concept trends are similar. As shown in Fig. 16, the optimum number of harvests per year is shifted towards 10, as the M&R cost variation is more important in this case. An optimum number of cycles before adsorbent replacement of 30 to 40 can be seen in Fig. 17, with a minimum specific cost of \$350/kg-U.

Finally, changing the loop length from 100 m to 200 m would reduce the cost from \$403/kg-U to \$381/kg-U, as shown in Fig. 18.

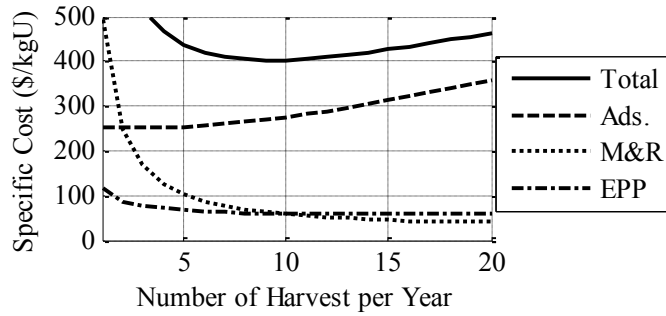


**Fig. 16 Specific Cost for the symbiotic concept as a function of the number of harvests per year (18 cycles before replacement of the adsorbent)**

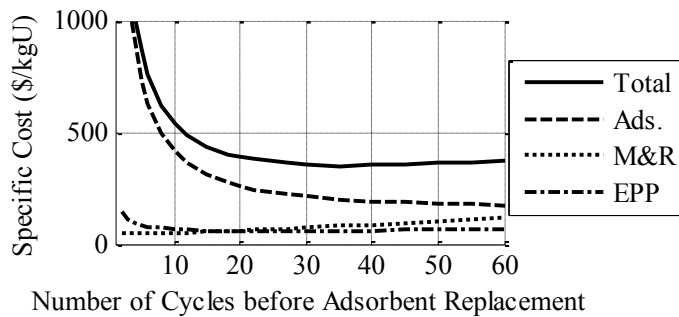


**Fig. 17 Specific Cost for the symbiotic concept as a function of the number of cycles before replacement of the adsorbent (10 harvests per year)**

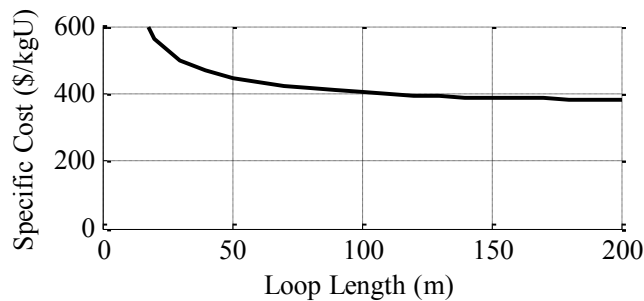


**Fig. 18 Specific Cost for the symbiotic system as the function of the loop length**

From the present cost analysis, it seems reasonable to assume that both concepts can eventually produce uranium under the market price, as the adsorbent gets better and the cost of producing terrestrial uranium increases. Although the 3D net concept appears to provide slightly lower cost due to its economy of scale, the authors believe that the symbiotic system is advantageous in several ways. Symbiotic operation with wind farms removes the need for finding additional offshore sites and makes it scalable from a turbine to the wind farm. Furthermore, the large number of components would lend itself to automated manufacturing and hence the costs could be significantly lower. It further benefits from the improvement in life time and kinetics of adsorbents. For example, an adsorbent with 1% degradation per cycle, 4 g-U/kg-ads capacity and a time constant of 5 days would reduce the cost to \$80/kg-U with 50 harvest per year and 150 cycles before adsorbent replacement. The effect of varying adsorbent capacity and degradation per cycle is shown in Fig. 19 for a time constant of 5 days, based on the current adsorbent kinetics, and a maximum adsorbent lifetime of 3 years. The cost of uranium is given for the optimum number of harvest for every point. Number of harvest per year is limited to 50 in this analysis.

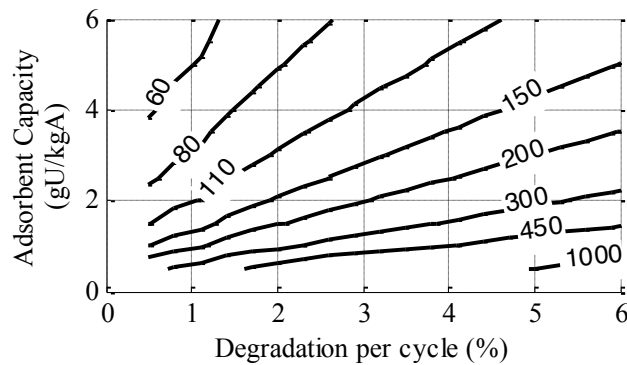


**Fig. 19 Specific uranium cost (\$/kg-U) against adsorbent capacity and degradation per cycle for a time constant of 5 days and a lifetime of 3 years**

## VII. CONCLUSIONS

In this study two concepts to reduce the price of recovery of uranium from seawater using braided line polymer adsorbent were proposed: a stationary and a continuous system. In the stationary system one ship recovers a 3D net of braided line adsorbent, performs elution on board and redeploys the net without the need to return to shore. The second concept was designed to be fixed to an offshore wind turbine structure at the waterline and continuously run the adsorbent from seawater to an elution process on the turbine platform and back to the seawater thus allowing adjustment of the duration of the adsorption/elution cycle.

First order engineering and economics analysis were conducted to evaluate the feasibility and cost competitiveness of the concepts. The stationary design was found to greatly reduce the mooring and recovery operations cost thanks to an optimized one ship operation and a high adsorbent/anchoring weight. The cost of U production with this system was estimated at \$326/kg-U, which constitutes a large improvement over existing systems. By shortening the harvest period the continuous concept was able to increase the adsorbent yield while achieving reduction of mooring and recovery costs though not as significant as for the stationary system. An analysis of this system shows that the cost of U production is expected to be about \$403/kg-U, which again compares favorably with existing systems.

The continuous concept was selected for the construction of a prototype even though its production price is higher because it presented several advantages. The development of more durable and selective adsorbent would reduce the penalty from more frequent elution (chemical degradation). This would greatly advantage a continuous system since shorter duration of the adsorption/elution cycle with higher adsorbent yield would become optimal. In addition this system is scalable from one offshore wind turbine to an entire wind farm, help making ocean utilization more efficient by providing more energy harvested from the same ocean surface. In addition, mass manufacturing economies of scale are likely to drive down the costs for this system.

## **ACKNOWLEDGMENTS**

The authors would like to thank Dr. Richard Garwin for posing the initial problem to us. Dr. Ronald Campbell provided advice on economic analysis and concept development. Dr. Charles Forsberg provided us with background and information on the early work in this area of Prof. Michael Driscoll, and very helpful comments on the figures. This work was conducted as a term project in MIT course 2.75 (<http://web.mit.edu/2.75>). Support for this project was provided from the S. D. Bechtel, Jr. Foundation and the MIT Energy Initiative.

## REFERENCES

1. “Uranium 2011: Resources, Production and Demand,” A Joint Report by the OECD Nuclear Energy Agency and the International Atomic Energy Agency, Organisation for Economic Co-operation and Development (2012).
2. C. W. FORSBERG, P. F. PETERSON, and P. S. PICKARD, “Molten-salt-cooled advanced high-temperature reactor for production of hydrogen and electricity,” *Nucl. Technol.*, **144**, 3, 289 (2003).
3. K. OGUMA, T. SUZUKI, and K. SAITO, “Determination of uranium in seawater by flow-injection preconcentration on dodecylamidoxime-impregnated resin and spectrophotometric detection,” *Talanta*, **84**, 5, 1209 (2011).
4. M. TAMADA, “Current status of technology for collection of uranium from seawater,” *42nd Session of the Erice International Seminars on Planetary Emergencies*, August 19–24, 2009.
5. R. V. DAVIES, J. KENNEDY, R. W. MCILROY, R. SPENCE, and K. M. HILL, “Extraction of uranium from seawater,” *Nature*, **203**, 4950, 1110 (1964).
6. J. KIM, C. TSOURIS, R. T. MAYES, Y. OYOLA, T. SAITO, C. J. JANKE, S. DAI, E. SCHNEIDER, and D. SACHDE, “Recovery of Uranium from Seawater: A Review of Current Status and Future Research Needs,” *Sep. Sci. Technol.*, **48**, 3, 367 (2013).
7. A. ZHANG, T. ASAKURA, and G. UCHIYAMA, “The adsorption mechanism of uranium (VI) from seawater on a macroporous fibrous polymeric adsorbent containing amidoxime chelating functional group,” *React. Funct. Polym.*, **57**, 1, 67 (2003).

8. T. S. ANIRUDHAN, A. R. THARUN, S. RIJITH, and P. S. SUCHITHRA, "Synthesis and characterization of a novel graft copolymer containing carboxyl groups and its application to extract uranium (VI) from aqueous media," *J. Appl. Polym. Sci.*, **122**, 2, 874 (2011).
9. N. SEKO, A. KATAKAI, S. HASEGAWA, M. TAMADA, N. KASAI, H. TAKEDA, T. SUGO, and K. SAITO, "Aquaculture of uranium in seawater by a fabric-adsorbent submerged system," *Nucl. Technol.*, **144**, 2, 274 (2003).
10. M. KANNO, "Present status of study on extraction of uranium from sea water," *J. Nucl. Sci. Technol.*, **21**, 1, 1 (1984).
11. R. VAN REIS and A. ZYDNEY, "Bioprocess membrane technology," *J. Membr. Sci.*, **297**, 1, 16 (2007).
12. G. A. TULARAM and M. ILAHEE, "Environmental concerns of desalinating seawater using reverse osmosis," *J. Environ. Monit.*, **9**, 8, 805 (2007).
13. T. SUGO, M. TAMADA, T. SEGUCHI, T. SHIMIZU, M. UOTANI, and R. KASHIMA, "Recovery System for Uranium from Seawater with Fibrous Adsorbent and Its Preliminary Cost Estimation," *J. At. Energy Soc. Jpn.*, **43**, 10, 1010 (2001).
14. M. TAMADA, N. SEKO, N. KASAI, and T. SHIMIZU, "Cost estimation of uranium recovery from seawater with system of braid type adsorbent," *Trans. At. Energy Soc. Jpn.*, **5**, 4, 358 (2006).
15. D. J. SACHDE, "Uranium Extraction from Seawater: An Assessment of Cost, Uncertainty and Policy Implications," Master's Thesis, The University of Texas at Austin (2011).
16. M. TAMADA, N. SEKO, and F. YOSHII, "Application of radiation-graft material for metal adsorbent and crosslinked natural polymer for healthcare product," *Radiat. Phys. Chem.*, **71**, 1, 223 (2004).

17. W. RUDZINSKI and W. PLAZINSKI, “Kinetics of Solute Adsorption at Solid/Solution Interfaces: A Theoretical Development of the Empirical Pseudo-First and Pseudo-Second Order Kinetic Rate Equations, Based on Applying the Statistical Rate Theory of Interfacial Transport,” *J. Phys. Chem. B*, **110**, 33, 16514 (2006).
18. N. SEKO, A. KATAKAI, M. TAMADA, T. SUGO, and F. YOSHII, “Fine fibrous amidoxime adsorbent synthesized by grafting and uranium adsorption–elution cyclic test with seawater,” *Sep. Sci. Technol.*, **39**, 16, 3753 (2004).
19. T. SUZUKI, K. SAITO, T. SUGO, H. OGURA, and K. OGUMA, “Fractional Elution and Determination of Uranium and Vanadium Adsorbed on Amidoxime Fiber from Seawater,” *Anal. Sci.*, **16**, 4, 429 (2000).
20. “Guide for the Certification of Offshore Mooring Chain,” American Bureau of Shipping (2009).
21. “Consumer Price Index:” <ftp://ftp.bls.gov/PUB/special.requests/CPI/cpi.ai.txt> (current as of Oct. 24, 2013).
22. K. CULLINANE and M. KHANNA, “Economies of scale in large container ships,” *J. Transp. Econ. Policy*, 185 (1999).
23. “Occupational Employment Statistics:” [http://www.bls.gov/oes/current/oes\\_nat.htm](http://www.bls.gov/oes/current/oes_nat.htm) (current as of Oct. 24, 2013).
24. “Commercial Marine Emission Inventory Development,” EPA420-R-02-019, Assessment and Standards Division Office of Transportation and Air Quality, U.S. Environmental Protection Agency (2002).
25. “Correlations from Plant Design and Economics for Chemical Engineers:” <http://www.mhhe.com/engcs/chemical/peters/data/ce.html> (current as of Oct. 24, 2013).

## APPENDIX A. PROOF-OF-CONCEPT PROTOTYPE

A 1:50 scale bench-top prototype was built to study the feasibility of the continuous strategy, with cables replacing the absorbent net (Fig. 20). The prototype objective is to demonstrate that: (1) the continuous system can be driven by a single motor, (2) slip between the pulleys and cables can be avoided, and (3) entanglement of the cables can be avoided under turbulence in water. The prototype was tested both on land and in the MIT swimming pool in the Zesiger Sports Center.

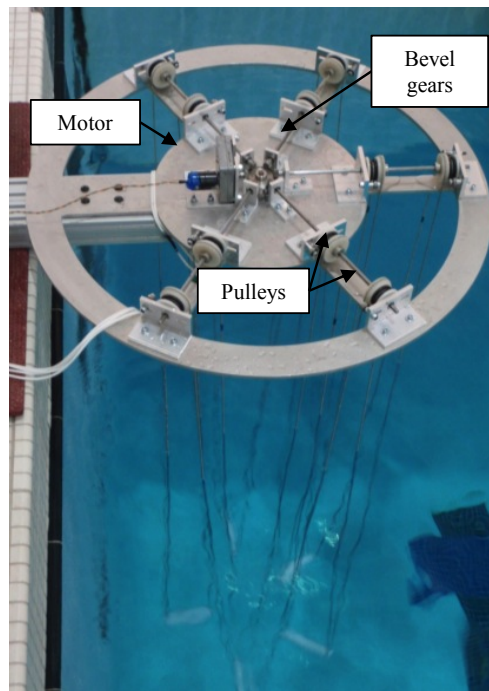


**Fig. 20 Prototype testing in MIT swimming pool**

The system is mounted 28” diameter aluminum plate cut using an OMAX Abrasive Waterjet Machining Center. Torque from the DC motor is transmitted to the five pulley-cable assemblies (Fig. 21) through using bevel gears. Rope linear velocity was increased to 4 cm/s to maintain a similar Reynolds to the large scale system.

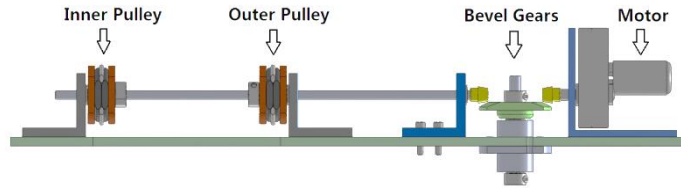


**Fig. 21 Shaft assembly and motor**

On each shaft, two sets of cable-pulley systems are installed, as seen in Fig. 22. Two cable-pulley systems were tested, as the choice of this system is crucial in the design of the actual system. One set of the cable-pulley systems consists of pulleys and nylon ropes (ropes not shown in the picture), chosen for its low-cost. The second set consists of bead belts and bead-belt sprockets that would be more expensive, but more reliable due to the use of positive action. In each of the systems, one cable goes around the outer ring of pulleys and the other go around the inner ring. The two cables form five pairs of parallel loops and stretch 2 m below the platform. The 2 m long loops represent 100 m long adsorbent nets in the actual system according to the 1:50 scale.



**Fig. 22 Shaft with pulleys and bead belt sprockets**

### **Regular pulleys and ropes**

For the pulley and rope system, two rubber O-rings were placed in the groove of each pulley, to increase the traction coefficient. The rope is placed on the pulley the between the O-rings. Pinching rollers are used to press the ropes against the O-rings to further increase traction. The degree of pinching can be adjusted by adjusting the position of the pinching rollers on the aluminum bracket supporting the shafts (Fig. 23).

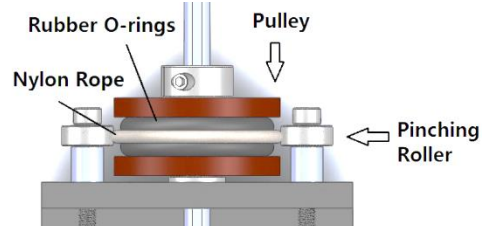


**Fig. 23 Pulley, rope and pinching rollers**

Rollers at the bottom of the loops help separate the inner and outer ring loop by placing them in their two grooves and tension the ropes with their weight (Fig. 24). A hole through the center axis of each roller allows additional weights to be attached without hindering the motions of the ropes.



**Fig. 24 Bottom rollers**

The weights that hang on the rollers were designed not only to adjust tension in the ropes but also to maintain the length of each loop. This is achieved by attaching one weight to two adjacent rollers (Fig. 25). In this arrangement, if one roller is higher, it will lift the weight and loosen the connection between the weight and the adjacent roller. Consequently the weight is supported by the high roller only instead of being distributed between two rollers. The increased vertical load brings the roller back down through small amount of slip in the pulleys until loop lengths equalize. This arrangement makes the system stable with regards to loop length.

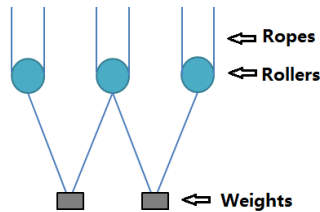


**Fig. 25 Weight connection**

Regular pulley and rope configuration was first tested on land with each weight hanging under one roller rather than attached between two rollers as seen in Fig. 26. The rollers were adjusted to lie in a horizontal plane before the system was run. After running the motor for 6 minutes, the rollers moved to different heights because of either slip between the ropes and the pulleys or differences in pitch diameter between the pulleys. The results showed that this configuration was not stable.



**Fig. 26 Rollers with individual weights initial position (left) and after 6min (right)**

The second test was conducted with weights connected to two adjacent rollers, as shown in Fig. 25. The results show that this configuration is stable. Both tests on land and in the swimming pool showed that the rollers would remain level after 6 minutes of running. To further test the robustness of this configuration, a test was done in the swimming pool starting with one roller about 2 inches higher than the others. As can be seen in Fig. 27, after 1 minute of operation, because it directly supported one weight the top roller was lowered and the differences in roller heights came back to an equilibrium position.

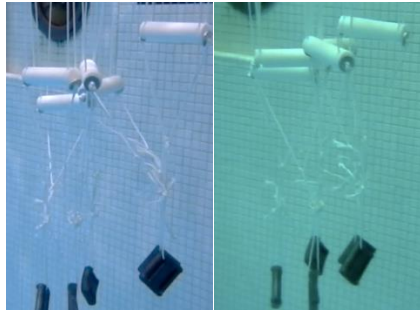


**Fig. 27 Testing system stability  
initial position (left) and after 1min (right)**

Finally, the system with its connected weights configuration was submitted to horizontal currents. The current was generated by kicking in place by a diver wearing fins. The results showed that the system was able to sustain moderate currents and the roller remained level after 3 minutes of horizontal current test.

### **Bead belts and bead-belt pulleys**

For the second system, the bead belts use 4mm stainless steel beads. The sprockets have hemispherical grooves that lock to the beads that avoid slip by providing positive action. Although not as essential as in the pulley-rope system, the bottom rollers can be used for this configuration.

The bead belts with rollers configuration was tested both on land and underwater. Both tests indicated that the system was able to operate without any slip. Figure 28 shows the underwater test. The rollers remained level after 1 min and 5 min of operation. The results proved that the bead belt system is stable under continuous operation.

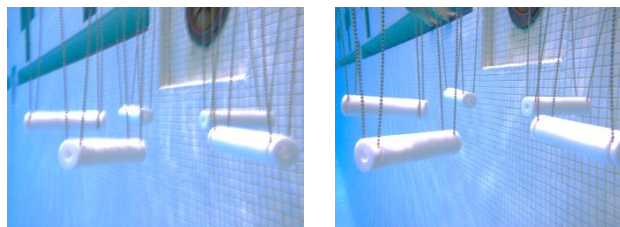


**Fig. 28 Bead belt stability – 1min (left) and 5 min (right)**

The bead belt configuration was also tested under horizontal current condition. The current generated large motions of the rollers and bead-belts. The configuration of bead belts with rollers was found to be less stable than the weighted ropes. However, the system was still able to sustain moderate currents with the rollers staying in positions. The rollers were helpful to prevent bead belt entanglement. Under larger currents, the movements of the bead belts became so large that some rollers fell out of their loops. Connecting some weights to the rollers would decrease the amplitude of their motion. In addition, the rollers could also be interconnected to form a lower platform which would also increase resistance to currents.

## **Conclusions**

A 1:50 scaled down prototype of the continuous system was tested in a pool and validated that it can operate reliably in an aquatic environment. It was found that additional mechanism to maintain stability is required if the system relies on friction to drive the adsorbent lines. Positive action (bead belts) made the system stable with regards to length of adsorbent loops. The prototype was able to resist moderate cross flow currents. Additional efforts would be needed to increase robustness and avoid adsorbent entanglement, such as creating a monolithic lower platform for the rollers at the bottom loops of the adsorbent lines. To further evaluate this concept proving the feasibility of continuous elution through testing and analysis will be an important step.